Polyamide powder coating of copper substrates: Impact of process parameters on the surface properties, the adhesion strength and the interface microstructure

Célia Badji, Ahmed Allal, Jean-Charles Dupin, Frédéric Léonardi

Polyamide powder coating of copper substrates: Impact of process parameters on the surface properties, the adhesion strength and the interface microstructure

Abstract

The aim of this work was to assess the impact of coating process parameters on the quality of biopolyamide coating on copper substrates obtained by conventional hot dipping fluidized bed coating process (CHDFB). The experiments carried out in this study allowed to understand the decohesion mechanism of virgin biopolyamide 11 before having assessed coating properties by chemical, mechanical and microstructural characterizations. The investigations showed that a higher thickness and better surface finishing were obtained for high preheating temperatures and intermediate immersion times mainly thanks to a higher heat energy stored by the metal support whereas long immersion times compromised the aspect. A laboratory-developed mechanical test was also carried out to determine the adhesion strength. This allowed to overcome the variability linked to the analyzed surface preparation or the local radius of curvature of pull-off and peel conventional adhesion tests respectively that could influence the adhesion strength data. It was concluded that, even if more severe metal preheating conditions improved the coating physical properties, they led to a worse adherence. Surface morphology and spectrometry analyses of the coating side facing the interface correlated to the mechanical test results allowed to highlight the growing formation of copper oxide and copper hydroxide compromising the coating adhesion. From all the results, the optimal process parameters were determined.

Keywords : fluidized bed, adhesion, polyamide 11, oxidation, coating, metal

1. Introduction

Today, surgical instruments are mainly made of stainless steel. For open-heart operations, the contacts between the steel instrument such as the sternal spacer or heart spacer and soft tissues such as the heart or chest can be traumatic. The idea is to replace these very hard instruments by softer instruments with two objectives: 1) have a softer instrument/organ contact to reduce the traumas hence the coating of the metal by a polymer with high thickness; 2) have an adaptative instrument to the patient's organs and body in order to go towards "tailor-made" instruments; hence the use of copper parts instead of steel parts. The low modulus of copper allows the surgeon to fold it and adapt it to the patient.

The last two decades have seen the growth of the metal surface treatment and coating industry. Indeed, the coating of metal parts gives physicochemical properties specific to the application of the treated product (protection against corrosion, thermal performance, biocompatibility, etc.) allowing a wide range of end of uses of the product. This sector is undergoing a significant technological change in particular in response to environmental constraints which take an important part in the society [1]. Besides, the powder coating techniques, fluidized bed and electrostatic coatings, have been extensively studied since 1950s [2]–[4]. Indeed, contrary to solvent-based coatings that include emissions of Volatile Organic Compounds (VOCs) during process that can be harmful for the human health and the environment, those two techniques no needing solvent are eco-friendly [4]–[6]. More detailly, the fluidized powder bed technique is highly efficient, low time-consuming, and recent studies showed that this one presents a lower environmental impact that the electrostatic powder coating [5]. However, the conventional fluidized bed coating presents some limitations that are overcame with the electrostatic powder coating. Indeed, this last coating way does not need a preheating step at high temperature which reduces possible oxidative degradation of the coating polymer or the metal part [6]. Indeed, the generation of charged powder particles sprayed thanks to a gun onto the metal surface favors the adhesion of the coating. Also, contrary to the conventional fluidized bed coating, very thin films can be applied thanks to this method.

The choice of the coating polymer will depend on the expected properties of the final product. Polyamide coatings are characterized by their excellent durability, good flexibility with outstanding toughness, impact and abrasion resistance [7]. Among all the polyamide structures, most of the polyamide powders used for the metal coating are based on polyamide 11 (PA11). Contrary to the shorter chain length nylons, PA11 is issued from renewable resources [8] and presents a lower hygroscopicity than the first ones. Moreover, in the study brought in this paper, we selected a virgin biosourcedPA11 powder to perform the coating of the metal support in response to an industrial demand of a medical company which needed to develop a medical dispositive constituted of malleable copper part coated bioPA11. Thus, the adhesion of this biosourced polymer must be evaluated.

Studies done on the polyamide 11 powder fluidized bed coating of metallic supports used the polymer with additives (pigments, reinforcing fillers, fluidization additives …) [9]–[12]. Also, the use of primers or the modification of the metal surfaces (sand abrasion, paper abrasion, …) were investigated to enhance the coating adhesion on the metal workpieces without having characterized the interfacial adhesion and quantified the adhesion strength [7], [9], [11]. Whatever the way chosen to enhance the coating adhesion, it was mainly observed that as the preheating temperature increased, the coating thickness increased and the surface quality was improved [9], [13]. However, to our knowledge, any scientific study dealt with neat PA11 coating on metal substrates whereas information on its own coating behavior has to be provided.

Until today, peel or pull-off adhesion tests were performed to characterize and quantify the adhesion strength of polymer coatings on a substrate [14]. These mechanical tests are commonly used to assess the quality of coatings adhesion. However, in the case of peel tests, even if the bond failure proceeds at a control rate, the maximum load born by the coating is strongly dependent on the peeling angle and the local radius of curvature [15], [16]. For the pull-off adhesion tests, even if they are simple to perform and can be carried out in-situ [16], their limits mainly lie in the dolly misalignment that can induce the locus of failure shifting where the glue joining the dolly (the pull stub where the external force is applied) to the coating is thinnest [16]. Indeed, during the test, the coating pulled away from the metal support at a normal angle to the surface may be not completely taken off from all the tested surface and some plane failures appear. For instance, Takeshita et al demonstrated that during the mechanical test, failures were formed at three different breakage locations that were at the coating/metal, coating/dolly and metal/metal interfaces [14]. Thus, the recorded strength does not exclusively represent the adhesion strength at the coating/metal interface. Moreover, the maximum stress that can be applied may be limited by the cohesive strength of the coating or the strength of the coating-dolly bond. Also, the design of the dolly strongly affects the adhesion strength [18]. Otherwise, the adhesion strength of a polyamide coating obtained by fluidized powder bed coating has not yet been assessed. Hence, the study of the adhesion of neat polyamide being necessary, the main contribution of the paper is to give information on the coating performance of neat polyamide 11.

The main objective of this work is to give new insights in the coating behavior of virgin biopolyamide 11 without adding products or modifying metal surface of the substrate that ensure better adhesion as done in literature. The goal being to understand the decohesion mechanism of the neat coating, the impact of process parameters on the neat PA11 coating properties such as its thickness and its roughness was assessed. Then, the adhesion strength of non-additive PA11 on copper substrate was assessed by a method implying custom-made tools allowing to overcome the limits previously presented. Indeed, until today, conventional peel and pull-off tests are mostly used but greatly depends to factors presented hereafter that we will overcome in our work. Chemical and morphological analyses by spectrometry and microscopy measurements were brought to understand the mechanical performance variations according to the chosen process parameters.

2. Material and Methods

2.1 Material

The polyamide 11 powder (PA11), Rilsan Invent Natural grade, was supplied from Arkema (France). Even if this grade has not been specifically developed for metal coatings, this powder initially developed for laser sintering was chosen since the polymer is biosourced and classified USP class VI [19]. Copper cylinders with a diameter of 4.715 mm and a length of 70 mm supplied from Goodfellow (France) were

used as substrates. Acetone (Sigma Aldrich, purity of ≥ 99.5%) and acetic acid (Sigma Aldrich, purity of ≥ 99%) were used to remove organic contaminants and to remove the native oxide layers respectively.

2.2 Coating process

Before proceeding to the coating, the copper cylinders surface was firstly washed with acetone to remove the preservative oil from metal surfaces. Then, they were immersed in a stirred aqueous solution of acetic acid (10 vol%) to remove the copper oxide layer naturally present. Once done, the coating process consisted in a fluidized bed dipping during which the preheated copper part is immersed into the powder suspended by rising air flow. In contact with the hot metal part, the PA11 powder melts onto the metal surface and coats the metal. To perform the copper specimens coating, a 200 mm-inner diameter and 400 mm-height stainless-steel hopper connected to the air network was used. The airflow pressure was set at 0.25 bar. Three temperatures of copper specimens preheating (270, 300 and 320°C) were tested to examine the influence of this thermal process parameter on coating properties. The time of immersion in the fluidized bed varied from 1s to 12 s. The coating length was of 20 mm. Otherwise, in order to understand the evolution of the coating properties according to the temperature, the temperature variation outside the oven was followed with a Testo 868 thermal imaging camera for the 3 preheating temperatures. The infrared thermometer was pre-set at a thermal emissivity of 0.94. The coating thickness was determined by an outside micrometer allowing a non-destructive measurement on three areas of three specimens to consider the repeatability.

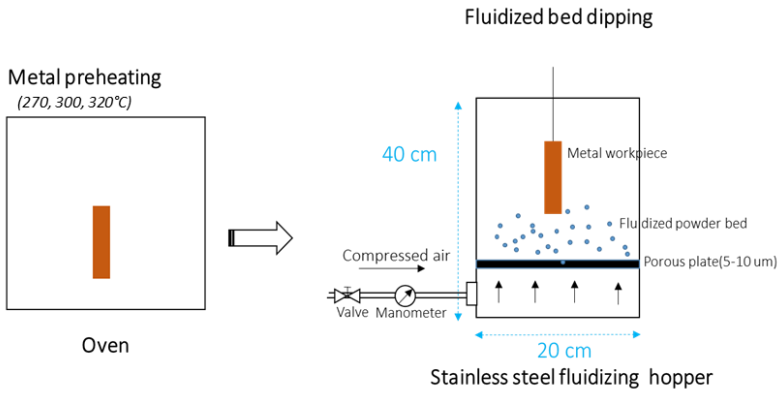

Figure 1 - Cartoon of the coating process (one-column fitting image)

2.3 Powder particle size distribution

Pictures of the powder particles were taken in transmission with a Leica Microsystems DM/LM microscope equipped with 20 optic and a Leica DFC280 video camera. The image treatments were performed on 1000 particles with ImageJ software.

2.4 Thermal properties of PA11

In order to determine the thermal properties of the PA11 powder, a Q100 Instrument calorimeter (TA Instruments, USA) was employed to determine its melting temperature Tm. The measurement was carried out under nitrogen atmosphere at a 20 mL.min^{-1} flow. The heating ramp ranged from 10°C to 220°C at 10°C.min^{-1} and preceded a cooling intermediate ramp from 220°C to 10°C at 10°.min^{-1}. The following figure indicates a melting temperature of the first heating step of 200°C. This suggests that the powder has to be heated above 200°C to be effectively in the melting state during the coating process. Also, the figure gives information on the crystallization. It occurs at 162°C. So the rearrangement of the polymer chains after melting occurs at this same temperature.

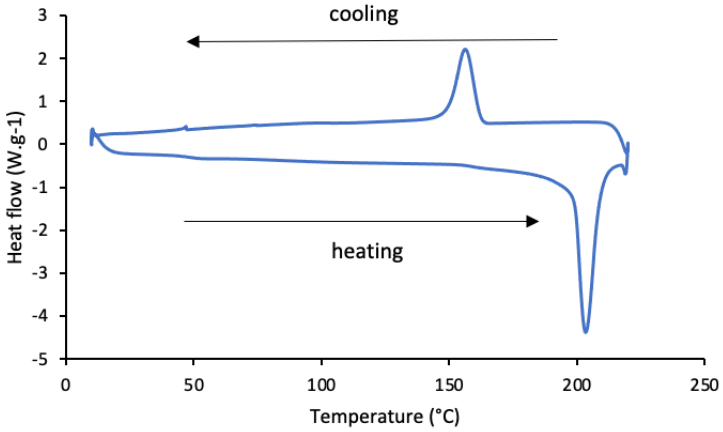

Figure 2 – PA11 DSC thermogram

2.5 Rheological properties of PA11

In order to determine the viscosity of the PA11, rheological analyses were carried out using a strain-controlled rotational rheometer (ARES by Rheometrics) in parallel plate geometry with a diameter of 25 mm. The dried powder of PA11 (4h at 105°C) were compressed in the melting state between plates at 220°C during 5 minutes in order to obtain disk sample of 25 mm of diameter and 2 mm of thickness. Small strain amplitude (2%) allows us to be in the linear viscoelastic regime. Frequency sweeps were performed at 180°C, 190°C and 200°C with frequency from 80 rad/s to 0.5 rad/s. Each isothermal experiment was done under nitrogen on a new sample in order to avoid rapid evolution of viscoelastic properties of PA11 sample. As mentioned in literature, post-condensation is the dominant thermal degradation mechanism in N_2 and post-condensation, chain scission and cross-linking simultaneously occur in air [20].

2.6 Roughness measurements

Since the surface aspect can give information on the coating homogeneity, a TR200 Time roughness measurement device was used to measure the arithmetic roughness parameter Ra (µm) of polyamide coatings according to the ISO 4287 standard:

$$Ra\ (\mu m) = \frac{1}{n}\sum_{i=1}^{n}|Zi| \qquad \text{Eq.1}$$

with Zi the vertical deviation according to the mean line (peaks and valleys) in µm, n the number of points along the analysed axis. Mean values and standard deviations were obtained from the analysis of three areas on samples.

2.7 Adhesion strength test

Peel test on copper cylinders to tear the PA11 coating was performed to measure the adhesion resistance of the polymer coating onto the cylindrical copper surface. Before mechanical test, the specimens were conditioned for 72h at 23 ±3 °C and 50 ±10 % of relative humidity. A MTS tensile test machine was used with a 1 kN load cell. The strain rate was set at 6 $mm.min^{-1}$ corresponding to shear rate chosen in literature for the shear test of polyamide/metal coating [21]. The cylindrical steel device that was used to determine the adhesion strength at the interface coating/copper part was fabricated (France) (Figure 3). Its scheme is represented in the Appendice section. This custom-made scraper was designed in order to solicit the interface between the polyamide coating and the copper substrate along the copper cylinder (shear test at an angle of 0° according to the surface in order to overcome the dependence of results on the radius of curvature implied by the peeling angle). A gap of 4.722-4.715 = 0.007 mm between the inner ring of the scraper and the copper cylinder was allowed to allow the introduction of the copper cylinder in the inner ring of the adhesion test device.

During the test, as the crosshead goes up, the coated copper cylinder clamped in the top jaw goes as well. The inner ring of the scraper, which is attached to the top of a hollow cylinder attached to the platform of the test machine and thus does not move during the test, only swipes along the neat copper cylinder at the beginning of the test. Therefore, no force is recorded since the inner diameter of the scraper roughly matches to the diameter of the copper cylinders (4.715 mm). Then, once arrived at the coating level, the scraper solicits the interface coating/copper part and a force (N) was recorded all along the test by the transducer. The test was videotaped through the hole present in the support to follow the physical response of the coating to the mechanical solicitation. The strength of adhesion (MPa) was also determined. Five replicate specimens of each material were tested.

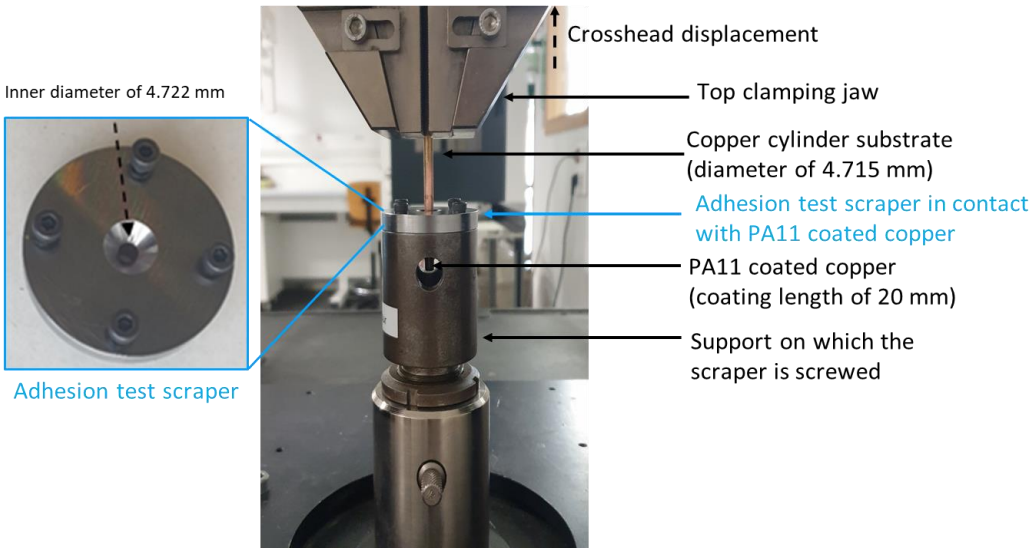

Figure 3 - Picture of the mechanical test bench

2.8 Surface morphology analysis

Once ripped from copper substrates after the mechanical test, the morphology of the polyamide coatings surface whose side was in contact with the copper substrate, was observed by scanning electron microscopy (SEM) HIROX SH-3000 (France) in order to understand the influence of the process parameters on the interface coating/metal debonding mechanisms. This coating side was metallized with gold using 30 mA for 60s (desk V, Denton Vacuum, USA). The accelerated voltage was of 25 kV.

2.9 Surface chemical analysis

As for the SEM analysis, X-Ray photoelectron spectrometry experiments of the ripped polyamide coatings surface whose side was in contact with the copper substrate have been achieved with a Thermo K-alpha spectrometer equipped with a hemispherical analyzer and a micro focused (400 µm diameter microspot) monochromatic radiation (Al Kα, 1486.6 eV) operating under a residual pressure of 1.10^{-9} mbar. Pass energy was adjusted to 20 eV. To compensate the charge effects occurring during the analysis, a dual beam charge neutralization system (low energy electrons and Ar^+ ions), which has the unique ability to provide consistent charge compensation was used. The calibration of all spectra was based on the binding energy of carbon 1s orbital at 285.0 eV. The mathematical fitting was done with the software Casa XPS using a least-squares algorithm and a non-linear baseline (Shirley). The experimental curves peaks were fitted using a combination of Gaussian (70%) and Lorentzian (30%) distributions.

2.10 Fourier Transform Infrared Spectroscopy analysis

A Perkin Elmer spectrometer operating in the Attenuated Total Reflectance (ATR) mode was used to follow the functional groups specific to the PA11 degradation to verify any eventual degradation of the polymer during the process. Thus, the band corresponding to the vibration of the carbonyl groups (1720

cm^{-1}) were particularly monitored. The device was equipped with a single reflection diamond crystal accessory. The two faces of the ripped off polyamide coatings (inner and outer) were analyzed, and the spectra were recorded as a result of the average of 32 scans in the 650 to 4000 cm^{-1} spectral range with a resolution of 2 cm^{-1}. Infrared spectra were normalized according to the Min-Max normalization method with the 2925 cm^{-1} reference band assigned to the CH_2 methylene groups.

3. Results and Discussion

3.1 Particle size distribution of PA11 powder

The particles shape of PA11 powder was observed by transmitted light optical microscopy (Leica, Microsystems). Also, the particle size distribution (PSD) was determined by digital image analysis on ImageJ software (Figure 4). The powder contains irregularly shaped rough particles with sharp edges having certainly resulted from a milling step [22]. Thus, since the diameter is not uniform and depends on the direction, we chose to determine the Feret's diameter of the particles, corresponding to the longest distance between any two points situated on the area perimeter (for 1000 particles on ImageJ) [23]. It can be noted that the PA11 powder particles present a dominant size range (Feret's diameter) between 20 and 30 µm. As indicated in the part 2.1, this powder has not been specifically developed for metal coatings. When comparing this value range corresponding to the longest distance of the non-spherical particles to the diameter of spherical particles of powders specifically manufactured for metal coatings, we conclude that these particles present a size substantially lower than the diameter of particles of powders usually used for metal coating carried out by conventional fluidized powder bed coating for which the dominant particle size ranges between 150 and 180 µm [9], [22]. Indeed, it is well-known that low coating thicknesses cannot be obtained through this coating method since the process parameters allowing to obtain a low thickness leads to surface defects and do not allow a continuous film [9]. This fact will be also verified hereafter in the paper.

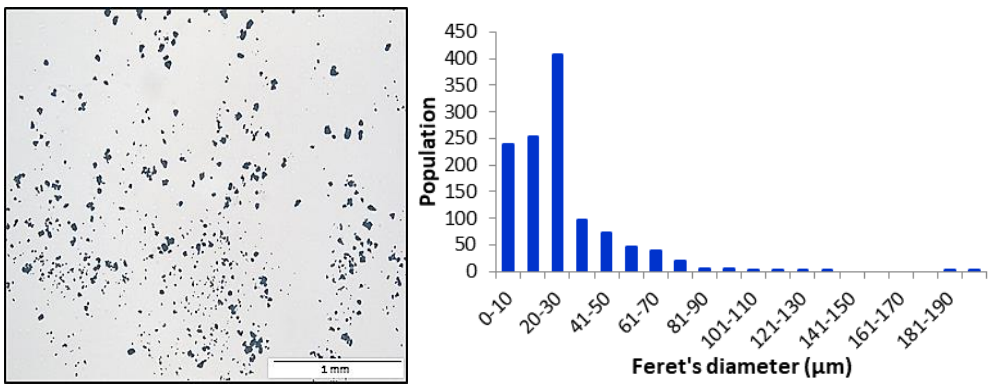

Figure 4 - Microscope image of PA11 particles (left) and particle size distribution (right)

3.2 Rheology properties of PA11 sample

Applying the Time Temperature Superposition principle, we built a master curve of the complex shear modulus at 180°C (Figure 5) with the three isothermal frequency sweeps. The zero shear viscosity is equal to 4200 Pa.s at the reference temperature. And then, using the thermal variation of the horizontal shift factor aT, we can obtain the activation energy of PA11 sample around 50-60 KJ.mol^{-1}. This value agrees with the literature [24] around 60 KJ.mol^{-1}. Considering the classical scaling law on zero shear viscosity ($\eta_o = kMw^{3.4}$) for linear entangled polymer, we can derive a weight average molar mass value of our sample at 48 Kg.mol^{-1} using the k value of Filipone et al for PA11 [20]. This molar mass Mw is in good agreement with values of the different PA11 grades studied by Okamba-Diogo et al from the same supplier [25].

Concerning the coating process, we can extrapolate the zero shear viscosity of the polymer at 270°C, 300°C and 320°C, one can found respectively 450 Pa.s, 250 Pa.s and 175 Pa.s. This rather low value for a polymer melt can explain the good coating of the metal part.

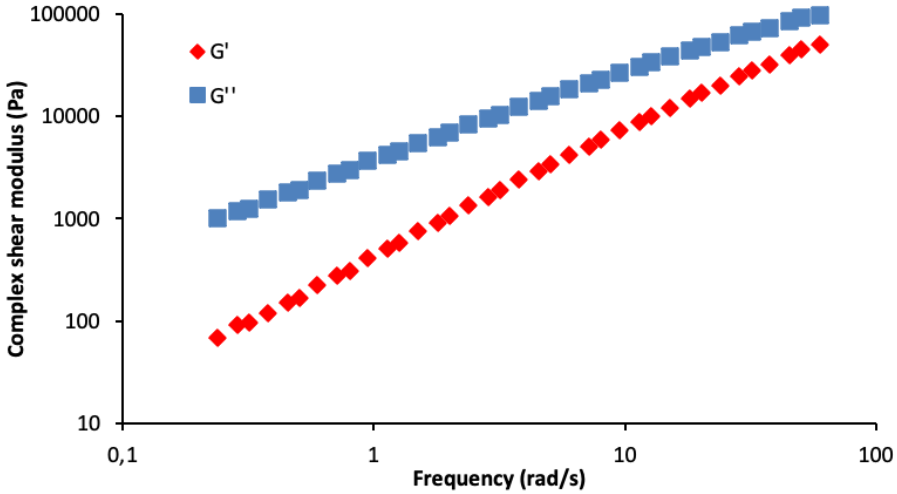

Figure 5 - Mastercurve of the complex shear modulus of PA 11 at a reference temperature of 180°C

3.3 Coating thickness

3.3.1 Impact of the process parameters on the coating thickness

The polyamide coating thickness was measured after different times of immersion in the fluidized powder (from 1s to 12 s) of copper specimens preheated to 270, 300 and 320°C. We firstly noted that the thickness increased with the time of immersion until reach a critical immersion time from which the coating thickness decreased. This trend was already observed in the literature and is explained by the aerodynamic and frictional forces undergone by the particles occurring at the metal surface due to airflow inducing the continuous mobility of powder particles [9] [26]. When the heat energy stored by the copper specimen is not enough to completely melt the polymer particles, the weakly adhering

particles on the surface are swept and brought away from the surface. These phenomena bring to a decrease of the coating thickness. Even if the same behavior is observed whatever the preheating temperature, this critical immersion time increased from 6s to 10s after copper preheating at 270°C and 320°C respectively. A complementary thermal analysis presented below of the data circled in the Figure 6 will allow us to understand the sudden fall of the coating thickness after a certain time of immersion and discuss the previous hypotheses.

Otherwise, for a same time of immersion, the coating thickness increased with the preheating temperature. For instance, after 6s of dipping, the thickness increased from 125 µm to 250 µm when the preheating temperature increased from 270 to 320°C, that is 2 times higher. This can be justified by the decrease of the melt viscosity of the powder with the temperature, giving rise to a continuous film and a higher thickness at a higher preheating temperature.

Also, the high standard deviations of results obtained when the metal was preheated to 270°C are certainly due to the presence of several defects and inhomogeneity because of the insufficient heat transfer between the metal substrate and the fluidized bed and the low thermal capacity of the copper substrate (385 $J.K^{-1}.kg^{-1}$) [27]. These hypotheses were verified by a monitoring of the temperature variations all along the process presented afterwards.

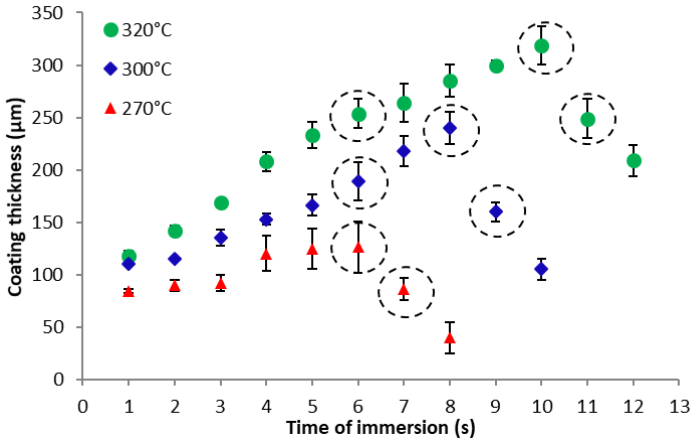

Figure 6 - Evolution of the coating thickness according to the time of immersion and the preheating temperature

3.3.2 Impact of the process parameters on the coating aspect

The melting property of the polymer powder greatly influences the coating properties after immersion of the preheated metallic substrate in the fluidized powder bed and highly depends on the temperature. Therefore, the evolution of the temperature of the copper cylinder support before and after dipping in the fluidized bed was monitored for the times of immersion situated in the sharp bend area corresponding to the data circled in the Figure 6 (Figure 7). We can firstly see that, once copper cylinders out of the oven, the dipping operation led to a significant drop of the copper surface temperature whatever the preheating temperature. Indeed, the fluidized powder bed being at 16°C, the temperature of the surface

of the preheated copper specimens suddenly dropped in contact with the fluidized particles. For 270°C preheating, the temperature of the coated copper after a dipping time of 6s is roughly equivalent to the melting temperature of the polyamide powder Tm of 201°C determined by Differential Scanning Calorimetry (DSC) (see part 2.4). This gave rise to the melting of all the powder particles having even weakly adhered to the surface i.e. the layer of particles furthest from the heated copper surface. However, after a dipping time slightly longer (7s), the temperature of the coated copper became lower than the melting temperature of the thermoplastic polymer (201°C) once out of the fluidized bed. Hence, the heat energy stored by the copper cylinder was no longer sufficient to sinter the powder particles and these particles were brought away from the metal substrate. Thus, this thermal study allowed to demonstrate that a synergetic effect between forces induced by the air flow exposed in the literature and the heat loss caused thinner coatings after long times of immersion.

After the cylinders preheating at higher temperatures (300 and 320°C) and short dipping times (less than 9s and 11s respectively), the surface temperature of the coating after immersion in the fluidized bed remained higher than Tm, inducing polyamide melting progress even once out of the oven (Figure 7). The temperature of the fluidized bed of 16°C was not so low to stop the melting. However, as for 270°C treatment, a coating thickness decrease was also observed after dipping times of 9s and 11s respectively after which the temperature was no longer higher than Tm.

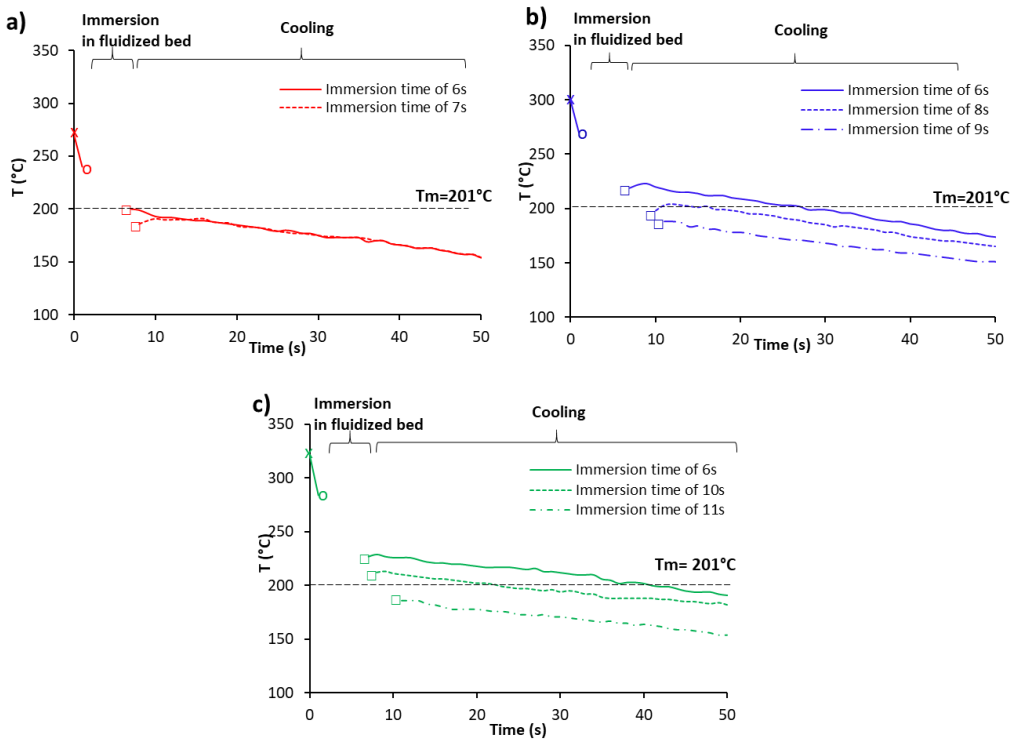

Figure 7 - Evolution of the temperature of coated copper parts preheated to 270°C (a), 300°C (b) and 320°C (c) over the time during the coating process (× : Temperature of the copper cylinder in the oven, o : Temperature of copper cylinder before immersion, □ : Temperature of coated copper cylinder once removed from the fluidized bed)

3.4 Coating roughness

The arithmetic roughness parameter values of the thermoplastic coating after the different process parameters are resumed in Figure 8. At 270° C, we can observe that after short immersion times (1s to 4s), the roughness value Ra of coatings exceeded the device limit value (> 40µm). This fact is explained by the presence of many coating defects because of the low number of powder particles having been allowed to contact the hot metal part after too short dipping times. Therefore, the particles coalescence has not been effective and pin holes were formed between melted particles. However, Ra distinctly decreased in the immersion time range 5s-6s before reacquiring non-detected values after longer times (>6s). This intermediate time interval permitted the powder to level into a continuous and smooth coating film. This period presented good thermal and timing conditions. Then, the heat loss after longer immersion durations compromised the surface aspect demonstrated by the high Ra value due to the presence of non-melted powder at the extreme surface. This gave rise to a powdery appearance.

After 300°C and 320°C thermal treatments of copper cylinders, even if the short times of copper immersion in the polyamide powder bed also induced unacceptable roughness values (Out Of the measurement Range (OOR)), the roughness decrease was noted after shorter immersion times and in an intermediate range of interest wider than for 270°C preheating (from 3s to 7s at 320°C). Thus, in this case, increasing further the dipping time caused a growth in the coating thickness without deteriorating the surface finishing. Indeed, it is easily understood that the higher preheating temperature allowed the copper specimens to remain longer at a temperature higher than Tm. Also, we can observe that values of Ra at those two higher temperatures gave rise to smoother surfaces than at the lower temperature of 270°C for same immersion times. Then, after 9s for 300°C and 11s for 320°C, Ra increased to values beyond 40µm. These observations are in consistence with the coating thickness evolution since this sudden second increase of the roughness from 2.15 µm and 1.95 µm to an OOR value (>40 µm) for 300 and 320°C respectively coinciding with the sharp variation trend change of the thickness evolution (Figure 6) can also be accounted for the significant heat loss after long dipping times.

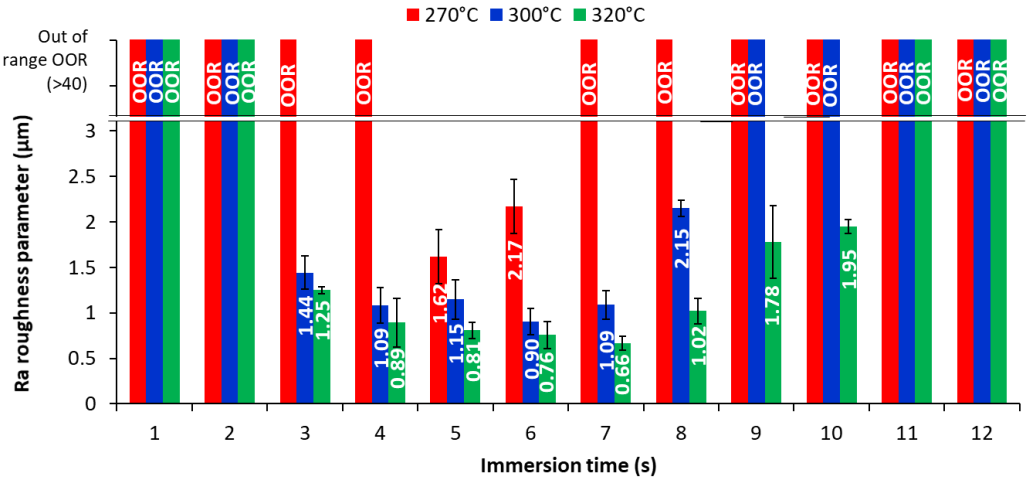

Figure 8 - Variation of Ra roughness parameter according to the immersion time for 270°C (red), 300°C (blue) and 320°C (green) copper preheating temperatures

3.5 Interfacial adhesion strength

3.5.1 Impact of preheating temperature and immersion time

In the Figure 9, the load needed to pull out the PA11 coating from the copper specimen is represented as a function of the displacement of the crosshead, i.e. the displacement of the scraper which solicits the coating/metal interface (see Figure 3). The mechanical properties were investigated for three different times of immersion (3s, 5s and 6s). Pictures of polyamide coated copper specimens at different moments of the mechanical test for the intermediate immersion time of 6s are consigned in Figure 10. The scheme of the behavior of the coatings during the mechanical test are also illustrated in this same Figure.

We firstly noted that, for a same preheating temperature, the mechanical profiles do not differ according to the immersion time (Figure 9). Indeed, in the initial range 0-0.7 mm of displacement of the scraper the specimen, a first maximum force (zone 1 in the graph) of 44±9N, 44±10N and 42±4N were noted for the coatings obtained at 270° C after immersion times of 3s, 5s and 6s respectively. Similarly, in the same displacement range, maximum forces of 58±11N, 66±15N and 57±9N were recorded for 300°C treatment and 109±6N, 104±6N and 113±11N for the same times of immersion after 320°C copper part treatment. However, the preheating temperature strongly influenced the mechanical response in this same displacement range. By observing the behaviors of the polyamide coatings during the test (Figure 10), we notice that this first peak corresponds to the load needed:

- To only remove a small upper part of the transparent coating carried out at 270°C and 300°C. Most of the lower coating part remained attached to the metal surface at this initial stage.
- To completely take off the 20-mm coating carried out at 320°C.

This observation suggests that the interface metal/coatings carried out at the two lower temperatures more resisted to the mechanical stress to which they were subjected. However, a higher temperature preheating (320°C) made the coating adhesion much worse since the entire 20-mm cylindrical coating

was peeled off at a low displacement and weakened the interfacial adhesion. After this decohesion of the coating from the metal surface, the coating carried out on copper preheated to 320 ° C only slipped on the surface of the copper part during the mechanical test. No interaction retained the coating to the metal surface, the load fell to 0 (zone 2). However, at 270°C and 300°C, once the 1st peak was exceeded, a 2nd maximum force was detected. By simultaneously examining the mechanical profile and the images, we noticed that at this moment, the partially peeled off coating was bending before folding over on itself. This is justified by the flexural properties of polyamide 11 [28]. Thus, this 2nd peak in the area 2 corresponds to the force needed to simply fold the partially peeled off upper part of the coating over. Finally, a 3rd step occurred during which the force reincreased and then remained constant. Indeed, after having folded, the adhesion test tool again solicited the interface coating/metal which was not stressed (lower part) while the coating progressively unfolded on itself until the end of the test to be completeley turned over at the end and completeley removed from copper. However, this stage is not of interest in this study of the interfacial adhesion since the force recorded includes both PA11/PA11 friction forces because of the coating folding and PA11 coating/metal decohesion force.

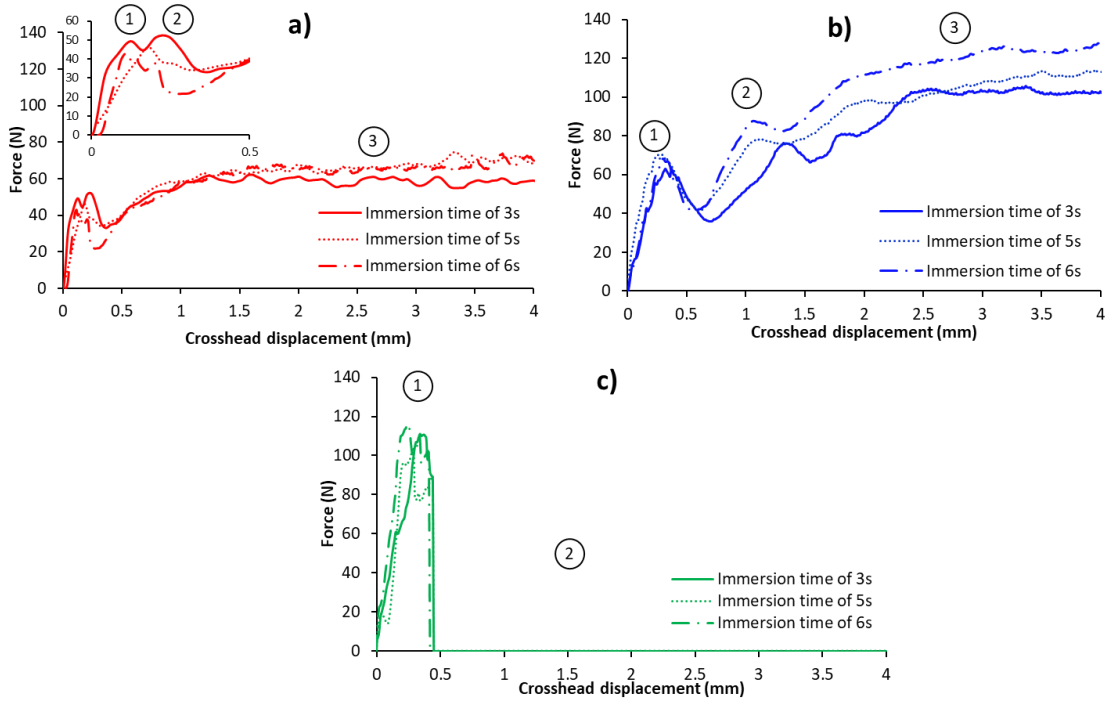

Figure 9 – Force versus displacement curves of PA11 coatings whose copper substrates were preheated to 270°C (a), 300°C (b) and 320°C (c)

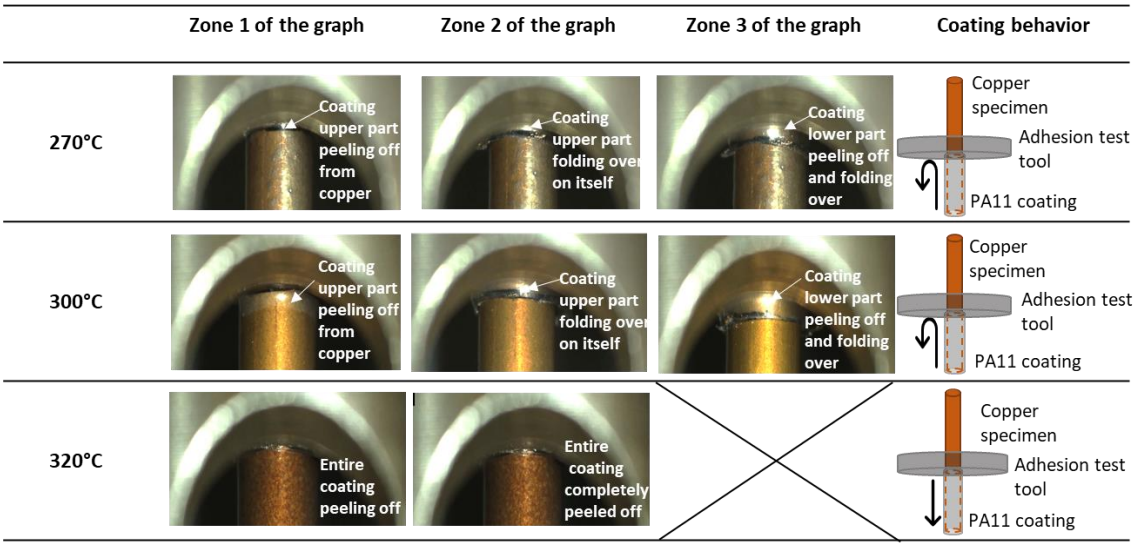

Figure 10 – Pictures of the PA11 coated copper specimens during the mechanical adhesion test (immersion time of 6s)

After having observed these results, we wanted to verify that the coating process (and more particularly the preheating step of the copper cylinders) would not induce thermo-oxidative degradation of the PA11 during the coating on the heated copper part at 320°C. As we can see in the figure of the Appendix (6.2 Infrared measurements), the band corresponding to the carbonyl group has not varied sufficiently between spectra of the outer (that was not in contact with the heated copper) and inner (that was in contact with heated copper) surfaces of the PA11 cylinder. This suggests that the heating of PA11 brought by the preheated copper part did not induce thermo-oxidation of PA11.

3.5.2 Determination of the adhesion strength

The interfacial adhesion strength was determined from the force needed to remove the peeled off upper part of the coating for 270°C and 300°C at a low displacement (first maximum load in zone 1) and the force needed to remove all the coating at 320°C (zone 1). Thus, we can calculate the strength S:

$$S = \frac{F}{A} \qquad \text{Eq.2}$$

with F the force applied to peel off the coating (N) and A the cross-sectional area (mm^2). Depending on the decohesion behavior of the cylindrical coating and the peeled off quantity, A can be calculated as followed:

$$A_{270°C} = 2\pi \times r \times d_{270°C} = = 2\pi \times 2.36 \times d_{270°C} \qquad \text{Eq. 3}$$

$$A_{300°C} = 2\pi \times r \times d_{300°C} = = 2\pi \times 2.36 \times d_{300°C} \qquad \text{Eq. 4}$$

with r the inner radius (mm) of the coating and the length of the coating upper part (mm) peeled off thanks to the maximum load firstly recorded in the first zone (low displacement). $d_{T(°C)}$ hence corresponds to the distance traveled after having snatched the coating uppert part and bended it. This displacement was indicated by arrows in Figure 9.

$$A_{320°C} = 2\pi \times r \times h = 2\pi \times 2.36 \times 20.0 \qquad \text{Eq. 5}$$

with r the inner radius of the coating and h the total peeled off coating length.

Results are resumed in Table 1. Even if the strengths are substantially comparable according to the immersion time, it decreased with the preheating temperature. Indeed, the average strength S drastically fell from 9.4 MPa to 0.36 MPa when the preheating temperature was decreased by 50°C.

Table 1 - Interfacial adhesion strength of coatings according to the immersion time and preheating temperature

Preheating temperature (°C)	270			300			320		
Immersion time (s)	3	5	6	3	5	6	3	5	6
Area of the peeled off coating A (mm^2)	5.41	5.05	4.33	22.97	20.01	19.56	296	296	296
Adhesion strength S (MPa)	9.1±1.7	9.1±1.2	9.9±0.9	2.9±0.48	3.5±0.75	3.5±0.46	0.37±0.0	0.34±0.1	0.38±0.1

Even if the higher temperatures preheating led to higher coating thicknesses and higher quality surface finishes, these process thermal conditions have compromised the coating adhesion performance. The morphological and chemical studies of the ripped off side of the coatings detailed hereafter were brought to investigate the decohesion mechanism.

3.6 Surface morphology of peeled off samples

The PA11 coating samples peeled off from the copper cylinders after the mechanical test were analyzed by scanning electron microscopy (SEM). Indeed, the surface morphology of the coatings whose side adhered to the copper cylinders preheated to the three different temperatures and immersed into the powder bed during 6s was observed (Figure 11). Firstly, the polyamide coating whose metal support was heated to 270°C presents a spade aspect, with a surface matter appearing to be soft with regular valleys and peaks. This was attributed to the thermoplastic material film deformation that was unstuck from the copper explaining the peeled appearance. However, a more inhomogeneous surface with a crumbled aspect was detected for 300°C due to relief lighter plates with sharp edges deposited onto the polyamide coating. This deposits part increased with the temperature until, at 320°C, this fraction almost entirely covered the polyamide thermoplastic material whose surface proportion decreased and whose soft and spade aspect is similar to that observed at 270°C (Figure 11 c)). The whiteness/grayness differences observed in the images b) and c) could bring overall information on elements composing the surface based on the composition contrast between the organic matter appearing dark gray (Carbon or Oxygen in polyamide 11) and the inorganic matter composed of heavier elements appearing lighter at the extreme surface in our case [29]. Indeed, the fraction of the extreme surface (relief plates) appearing lighter on SEM images and growing with the preheating temperature certainly corresponds to copper or copper oxide having come from copper specimens supports and having remained held to the coating. The chemical analysis of these surfaces by X-Ray photoelectron spectrometry (XPS) is necessary in order to affect the chemical nature of these products.

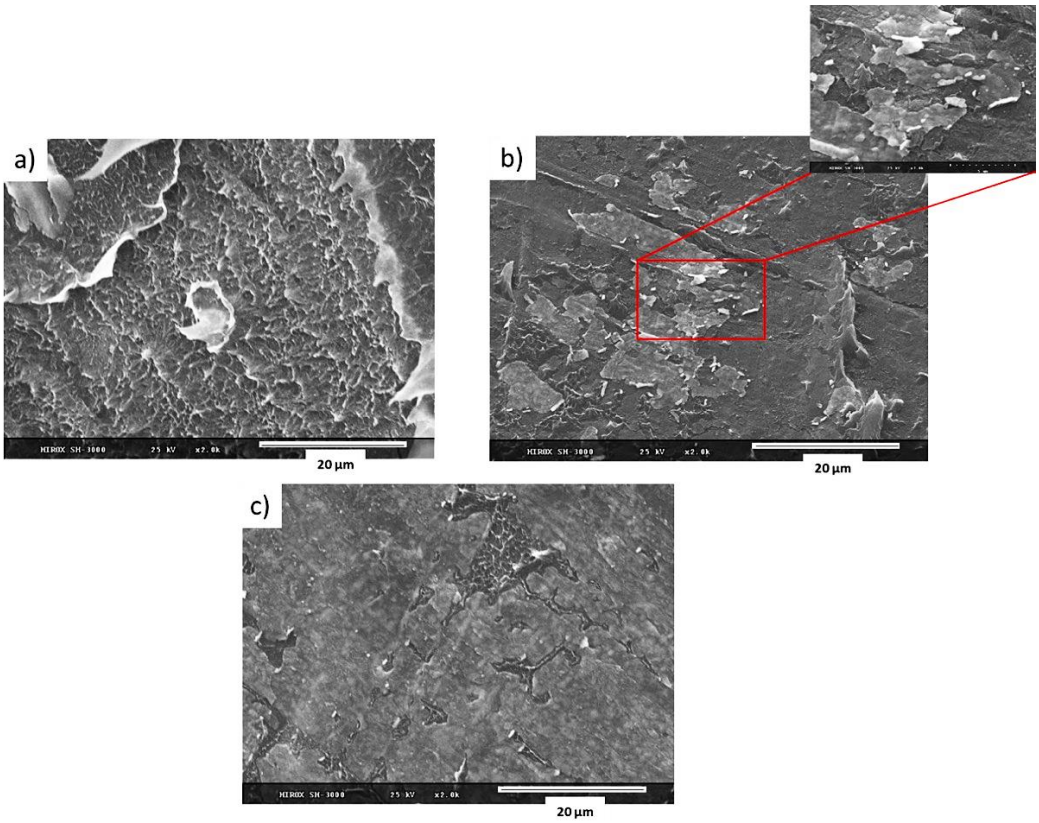

Figure 11 - SEM images of coating samples peeled off from the copper substrates preheated to 270°C (a), 300°C (b), 320°C (c) (immersion time of 6s)

3.7 Chemical analysis of the surface of peeled off samples

The surface composition of the coatings was studied by XPS. Following the previous results and assumptions made, the study was focused on the copper element (with the assumption of different oxidation degree, Cu(0), Cu(I) and Cu(II)) that was monitored in the Cu 2*p* spectra (binding energy range of 925-965eV) (Figure 12). No copper-based compound was identified on the coating specimen whose copper part was preheated to 270°C witnessed by the broadband background noise. At 300°C, the presence of Cu(I) specie is depicted due to the presence of the peak assigned to the $2p_{3/2}$ orbital at a binding energy of 932.7eV. This peak clearly revealed the presence of copper (I) oxide (Cu_2O) on the PA11 coating [30]. The formation of Cu_2O specie was probably due to severe copper preheating conditions explaining its absence in the spectra of coating samples whose copper substrate was preheated to 270°C [28]. During the mechanical test, this copper (I) oxide layer weakly adhering to the copper (0) cylinder remained attached to the thermoplastic coating. Also, the presence of the shake-up satellite peak found in the Cu 2*p* spectra (in the range 939-945eV) is an indication of the additional presence of Cu(II) species [32]. The literature dataset was used to affect the chemical structure to the copper-based phase having generated these peaks [30], [33]. Thus, the values of binding energies led us to attribute the peak detected at 935eV ($2p_{3/2}$) and the shake-up satellite peak at 939-945eV ($2p_{½}$) to copper (II) hydroxide $Cu(OH)_2$ specie. Indeed, $Cu(OH)_2$ could have been formed when the coatings were removed from copper

cylinders during the interfacial adhesion measurements. Copper hydroxide could have derived from Cu (s) or Cu_2O (s) formed in the oven due to the moisture present in the environment:

$$2\ Cu\ (s) + H_2O\ (g) + CO_2\ (g) + O_2\ (g) \rightarrow \mathbf{Cu(OH)_2\ (s)} + CuCO_3\ (s) \qquad \text{Eq. 6}$$

$$2\ Cu_2O\ (s) + 4H_2O\ (g) + O_2\ (g) \rightarrow 4\ \mathbf{Cu(OH)_2\ (s)} \qquad \text{Eq. 7}$$

Therefore, copper present on coatings is in a double chemical environment. Also, the intensity of the Cu 2*p* spectra peaks assigned to copper monoxide and copper hydroxide compounds grew up with the preheating temperature. We can suggest that as part of copper oxide increased, the interfacial adhesion became more brittle mainly because of copper oxide and copper hydroxide that came easily the pure copper cylinder off due to the weak mechanical strength of the oxide layer causing a sharp break of the interfacial adhesion at 320°C.

Otherwise, the atomic percentages of elements present at the surface of the coating samples (Table 2) were deduced from the normalization and the fitting treatments on the software CasaXPS. The quantitative analysis highlighted the preheating temperature effect with the related increase of the copper compounds concentration and confirmed the previous SEM data. Also, we can notice that Cu_2O and $Cu(OH)_2$ species are present in barely same proportions on the PA11 coating samples at 300°C whereas the Cu_2O phase is a little bit more pronounced than the $Cu(OH)_2$ one at 320°C. This could be assigned to the sharper adhesion break of the entire coating observed during the adhesion mechanical test obtained at 320°C than the one occurred at 300°C which took progressively place and allowed the progressive formation of $Cu(OH)_2$. In the same time, content of the organic matter of the polymer (valued from C1*s*, O1*s* and N1*s* peaks) is less significant with the temperature enhancement and the progressive residual stickness of Cu-based inorganic species.

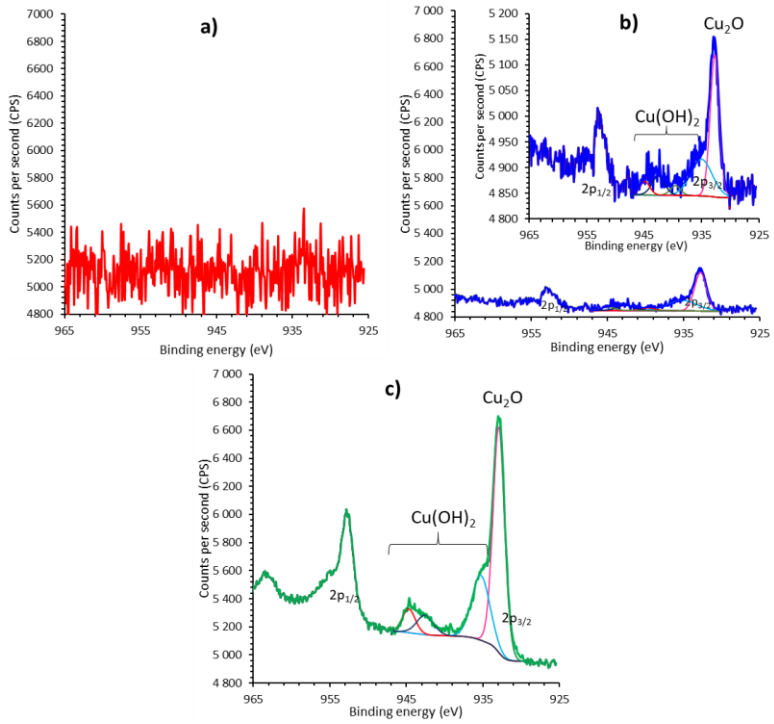

Figure 12 – Cu 2p spectra of coating samples peeled off from the copper substrates preheated to 270°C (a), 300°C (b), 320°C (c) (immersion time of 6s)

Table 2 - Chemical composition of the surface of peeled off coating samples (at%: atomic percentage) in the binding energy range 0-1400 eV according to the preheating temperature (immersion time of 6s)

	at%C (C *1s*)	at%O (O *1s*)	at%Cu (Cu *2p*)		at%N (N *1s*)
			at%Cu Cu_2O	at%Cu $Cu(OH)_2$	
270°C	80.2	15.9	-	-	3.9
300°C	73.9	21.9	0.04	0.04	4.1
320°C	75.0	20.2	0.22	0.17	4.4

4. Conclusions

In this paper, we study the conditions to obtain an efficient neat PA11 coating on copper cylindrical substrates using conventional fluidized bed coating. This study allowed to demonstrate that the higher the temperature of copper part preheating, the greater the coating thickness and the smoother the coating surface. Thus, according to the desired coating thickness, the time and the preheating temperature can be varied. However, the custom-made adhesion testing pointed out a strong effect of the temperature of the metal part preheating on the coating adhesion strength. Indeed, it was highlighted that even if increasing the copper preheating temperature allowed to promote the aspect and thickened the coating, it undermined the interfacial adhesion durability. The microscopy analysis allowed to notice different surface morphologies of the peeled off side of the coatings according to the preheating temperatures and it highlighted the presence of deposits after preheating of copper cylinders to the two higher preheating temperatures whereas preheating copper parts at lower temperature (270°C) preserved a neat polyamide 11 surface. The spectroscopy analysis used to determine the chemical composition allowed to give off the formation of copper oxide and copper hydroxide that grew up at the coating/Cu specimen interface and could have weakened the coating adhesion properties. The optimal parameters that were deduced from a compromise between the surface quality, the thickness and the adhesion strength are resumed in the following table. As reported previously, the highest preheating temperature (320°C) procured the highest coating thickness and the best surface finishing for a same time of immersion lots of surface defects were observed for coatings obtained at the lowest preheating temperature (270°C). On the contrary, the interfacial adhesion properties were greatly enhanced by decreasing the temperature from 320°C to 270°C. Based on these observations, it is difficult to select the best heating temperature. However, the intermediate preheating temperature (300°C) led to acceptable surface aspects (Ra roughness parameter < 2 µm for immersion times from 3s to 10s). Moreover, at this same preheating temperature, an immersion time of 6s allowed to reach a high enough coating thickness. Also, the mechanical test highlighted a mechanical behavior comparable to that obtained after preheating at 270°C even if the coating was slightly less adhesive. Thus, the resulting conditions chosen from these observations are resumed in the following Table.

Table 3 - Optimal process parameters

Preheating temperature (°C)	300
Time of immersion (s)	6

Finally, these results suggest to reduce the impact of the oxidation process on the metal surface by reducing the preheating temperature without compromising the surface aspect. Some perspectives are planned such as:

- preheating copper cylinder specimens in annealing conditions to prevent oxygen bad effects (under nitrogen)
- using a primer or structuring the metal substrate surface to promote the adhesion. This last suggestion can be conducted by laser engraving to modify the surface topography and enhance the coating mechanical anchoring to increase the polymer/metal adhesion properties.

Also, the same study driven by an electrostatic fluidized bed coating could preserve the copper part from the heating process and thus avoid the thermal degradation of the metal support.

Declaration of competing interest

The authors declare that they have no known competing financial interests or personal relationships that could have appeared to influence the work reported in this paper.

Acknowledgements

This work was supported by the program POCTEFA EFA313/19 LGMed.

5. References

[1] Thomas Westerkamp, “Paints and coatings that address environmental issues,” 2019.

[2] S. Al-Malaika, S. Andrews, and S. Andrzejewski, Processing and finishing of polymeric materials, Wiley., vol. 1. John Wiley & Sons, 2011.

[3] M. Barletta, G. Simone, and V. Tagliaferri, “A FEM model of conventional hot dipping coating process by using a fluidized bed,” Progress in Organic Coatings, vol. 54, no. 4, pp. 390–398, Dec. 2005, doi: 10.1016/j.porgcoat.2005.09.004.

[4] Z. Du, S. Wen, J. Wang, C. Yin, D. Yu, and J. Luo, “The Review of Powder Coatings,” Journal of Materials Science and Chemical Engineering, vol. 04, no. 03, pp. 54–59, 2016, doi: 10.4236/msce.2016.43007.

[5] K. Kellens, D. Paraskevas, W. Dewulf, and J. R. Duflou, “Environmental comparison of metal coating processes,” in Procedia CIRP, 2015, vol. 29, pp. 420–425. doi: 10.1016/j.procir.2015.02.179.

[6] M. Barletta, G. Bolelli, A. Gisario, and L. Lusvarghi, “Mechanical strength and wear resistance of protective coatings applied by fluidized bed (FB),” Progress in Organic Coatings, vol. 61, no. 2–4, pp. 262–282, Feb. 2008, doi: 10.1016/j.porgcoat.2007.09.029.

[7] Ö. F. Murathan and S. Kevran, “Investigation of thermal characteristic, surface morphology, mechanical properties and tribological properties of polyamide 11 powder coating,” Journal of Polytechnic, Apr. 2020, doi: 10.2339/politeknik.518540.

[8] H. Oliver-Ortega, J. A. Méndez, P. Mutjé, Q. Tarrés, F. X. Espinach, and M. Ardanuy, “Evaluation of thermal and thermomechanical behaviour of bio-based polyamide 11 based composites reinforced with lignocellulosic fibres,” Polymers, vol. 9, no. 10, Oct. 2017, doi: 10.3390/polym9100522.

[9] K. C. Leong, G. Q. Lu, and V. Rudolph, “A comparative study of the fluidized-bed coating of cylindrical metal surfaces with various thermoplastic polymer powders,” Journal of Materials Processing Technology, pp. 354–360, 1999.

[10] Arkema, “Safety data sheet of Rilsan Powder T - TYPE 1,” 2020.

[11] M. Guichenuy, J. F. Watts, M. L. Abel, A. M. Brown, M. Audenaert, and N. Amouroux, “Enhancement of the durability of a polyamide coating: Incorporation of an aminosilane into the powder formulation,” in Surface and Interface Analysis, Aug. 2004, vol. 36, no. 8, pp. 685–688. doi: 10.1002/sia.1736.

[12] M. Fernández-álvarez, F. Velasco, A. Bautista, F. C. M. Lobo, E. M. Fernandes, and R. L. Reis, “Manufacturing and characterization of coatings from polyamide powders functionalized with nanosilica,” Polymers, vol. 12, no. 10, pp. 1–20, Oct. 2020, doi: 10.3390/polym12102298.

[13] K. Leong, G. Lu, by J. Hartnett, and W. Minkowycz, “Heat transfer in fluidized bed coating of copper cylinders,” International Communications in Heat and Mass Transfer, vol. 20, pp. 699–710, 1993.

[14] Y. Takeshita, T. Sawada, T. Handa, Y. Watanuki, and T. Kudo, “Influence of air-cooling time on physical properties of thermoplastic polyester powder coatings,” Progress in Organic Coatings, vol. 75, no. 4, pp. 584–589, Dec. 2012, doi: 10.1016/j.porgcoat.2012.07.003.

[15] Y. Wang, “Thesis report: The effect of peeling rate and peeling angle on the peeling strength,” 2014.

[16] B. Duncan and L. Crocker, “Review of tests for adhesion strength,” NPL Report MATC(A)67, 2001.

[17] S. G. Croll, C. Siripirom, and B. D. Keil, “Pull-off adhesion test for coatings on large pipes: possible variations in failure location and mode,” 2014.

[18] J. F. Fletcher and Barnes D J, “Pull-off adhesion testing of coatings -Improve your technique.”

[19] Arkema Inc., “Rilsan® fine powders - Solutions for Laser Sintering - Invent polyamide powders for additive manufacturing.” [Online]. Available: http://www.arkema.com/en/products/productsafety/disclaimer/index.html

[20] G. Filippone, S.C. Carroccio, R. Mendichi, L. Gioiella, N.Tz Dintcheva and C. Gambarotti, Time-resolved rheology as a tool to monitor the progress of polymer degradation in the melt state – Part I: Thermal and thermo-oxidative degradation of polyamide 11, Polymer, Vol 72, Aug 2015, pp. 134-141

[21] “Technologies for economic and functional lightweight design.”

[22] L. Verbelen, S. Dadbakhsh, M. van den Eynde, J. P. Kruth, B. Goderis, and P. van Puyvelde, “Characterization of polyamide powders for determination of laser sintering processability,” European Polymer Journal, vol. 75, pp. 163–174, Feb. 2016, doi: 10.1016/j.eurpolymj.2015.12.014.

[23] “Feret’s diameter - ImageJ.” https://imagej.nih.gov/ij/index.html (accessed Dec. 21, 2021).

[24] L. Verbelen, S. Dadbakhsh, M. Van den Eynde, J-P. Kruth, B. Goderis and P. Van Puyvelde, Characterization of polyamide powders for determination of laser sintering processability, European Polymer Journal, vol 75, Feb 2016, pp.163-174

[25] O. Okamba-Diogo, Investigation of polyamide 11 embrittlement during oxidative degradation, Polymer, vol 82, Jan 2016, pp.49-56

[26] M. Barletta and V. Tagliaferri, “Influence of process parameters in electrostatic fluidized bed coating,” Surface and Coatings Technology, vol. 200, no. 14–15, pp. 4619–4629, Apr. 2006, doi: 10.1016/j.surfcoat.2005.04.030.

[27] M. Karahan and Ö. Kalenderli, “Coupled Electrical and Thermal Analysis of Power Cables Using Finite Element Method.” [Online]. Available: www.intechopen.com

[28] Arkema, “3D printing solutions - Rilsan® by Arkema - Thermoplastic powders for powder bed fusion,” 2018. [Online]. Available: http://www.arkema.com/en/products/product-safety/disclaimer/index.html

[29] Camp Wayne K, “Strategies for identifying organic matter types in SEM,” 2017. [Online]. Available: https://igs.indiana.edu/Coal/Macerals.cfm

[30] C. Zhu, A. Osherov, and M. J. Panzer, “Surface chemistry of electrodeposited Cu2O films studied by XPS,” Electrochimica Acta, vol. 111, pp. 771–778, 2013, doi: 10.1016/j.electacta.2013.08.038.

[31] M. Walkowicz et al., “Impact of oxidation of copper and its alloys in laboratory-simulated conditions on their antimicrobial efficiency,” Corrosion Science, vol. 140, pp. 321–332, Aug. 2018, doi: 10.1016/j.corsci.2018.05.033.

[32] M. C. Biesinger, “X-ray photoelectron spectroscopy (XPS) reference pages.” http://www.xpsfitting.com/ (accessed Nov. 25, 2021).

[33] W. Kautek and J. G. Gordon, “XPS Studies of Anodic Surface Films on Copper Electrodes,” Journal of The Electrochemical Society, vol. 137, no. 9, pp. 2672–2677, Sep. 1990, doi: 10.1149/1.2087008.

6. Appendices

6.1 Adhesion mechanical test

The following figure represents a scheme of the custom-made adhesion test device (scraper).

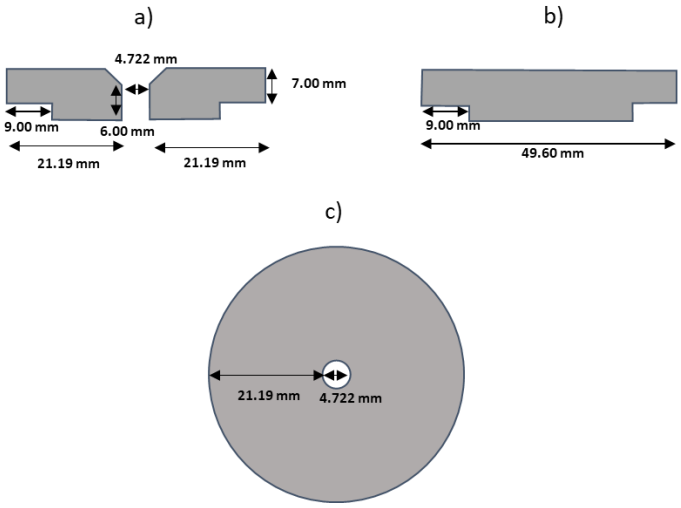

Figure 13 - Scheme of the adhesion test scraper used during the mechanical test soliciting the coating/metal interface (a) longitudinal section view, b) front view, c) top view)

6.2 Infrared measurements

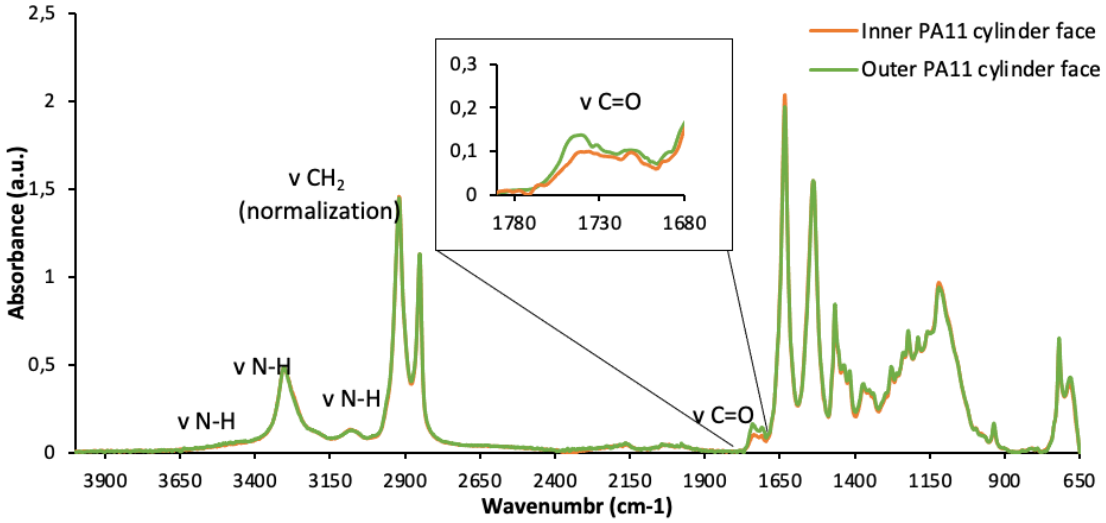

Figure 14 - Infrared spectra of the outer and inner faces of the polyamide cylinders ripped off after mechanical test